DIRAC 00-03

Monte Carlo Calculation of Pionium Breakup Probability

Cibrán Santamarina Ríos [a]

[a] *Universidade de Santiago de Compostela.*

A precise calculation of pionium breakup probability (P_{br}) in a target with a given Z is performed by solving the evolution equation system with a Monte Carlo method. The matrix elements of this system are calculated in the Born approximation making use of the dipole form factors. The results obtained are compared with those of the DIRAC technical proposal.

1 Introduction

The DIRAC experiment is dedicated to measure the pionium lifetime. In order to reach this goal a spectrometer is working at CERN specially designed to detect low relative momentum (q) $\pi^+\pi^-$ pairs. The yield of pair production at $q < 1\ MeV/c$ is the physical signal from which we can obtain the breakup probability (P_{br}) for pionium in a thin target foil (of the order of tenths of millimetre thickness). The breakup probability is a unique function of the pionium $1s$ state lifetime τ which we discuss in detail in this report. The lifetime measurement requires a precise knowledge of P_{br} as a function of τ. We have used a Monte Carlo technique to evaluate this function, as we describe in section 3, and we have checked the compatibility of this procedure with the results obtained in the technical proposal [1] and in [7] by L.G. Afanasyev.

2 Atomic production

The mechanism of pion atom production is the Coulomb interaction between $\pi^+\pi^-$ pairs in the reaction $p + A \rightarrow \pi^+\pi^- + X$ reaction [3]. The role of the π^+ π^- double inclusive production as the source of pions leading to a bound state of quantum number nlm is explicitly expressed in the pionium production

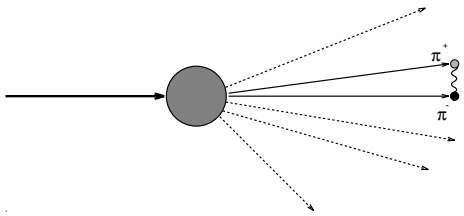

Fig. 1. *Production mechanism of pionium.*

cross-section:

$$\frac{\mathrm{d}\sigma^A(n,l,m)}{\mathrm{d}\mathbf{P}} = (2\pi)^3 \frac{E}{M} |\psi_{nlm}(\mathbf{0})|^2 \frac{\mathrm{d}\sigma_s^0}{\mathrm{d}\mathbf{p}_{\pi^+}\,\mathrm{d}\mathbf{p}_{\pi^-}}, \tag{1}$$

where the superscript 0 in the double inclusive cross-section indicates the neglect of Coulomb final state interactions and the subscript s takes into account that only short-lived sources can yield pion atoms. This double inclusive cross-section is evaluated for pions at equal momenta ($\mathbf{p}_{\pi^+} = \mathbf{p}_{\pi^-} = \mathbf{P}/2$). Hence, since hydrogen-like wave functions at origin verify:

$$|\psi_{nl}(\mathbf{0})|^2 = \begin{cases} 0 & \text{if } l \neq 0, \\ \frac{1}{a_\pi \pi n^3} & \text{if } l{=}0; \ ^1 \end{cases} \tag{2}$$

we see that only s states are created, with rate proportional to $1/n^3$.

2.1 A direct estimation of pionium spectrum from experimental data.

As explained in appendix A, equation (1) can be rewritten in spherical coordinates as:

$$\frac{\mathrm{d}\sigma^A(n,l,m)}{\mathrm{d}P\mathrm{d}\theta} = |\psi_{nl}(\mathbf{0})|^2 \frac{2^6(2\pi)^3}{M_A} \frac{E}{PP_t} \frac{\mathrm{d}\sigma_s^0}{\mathrm{d}P\mathrm{d}\theta\mathrm{d}P\mathrm{d}\theta}, \tag{3}$$

where the azimuthal angle dependence can be suppressed. This means that the atom spectrum can be obtained once the $\pi^+\pi^-$ double inclusive cross-section of $\pi^+\pi^-$ pairs from short lived sources is known. We have developed a procedure to make an estimation of this double inclusive cross-section making use of the DIRAC experimental data.

Hence we have chosen particle pairs within a time window of 0.5 ns. These pairs have a high probability of being emitted from the same $proton-nucleus$

[1] In this equation a_π is $A_{2\pi}$ Bohr radius: $a_\pi = \frac{2}{\alpha m_\pi} = 387 fm$.

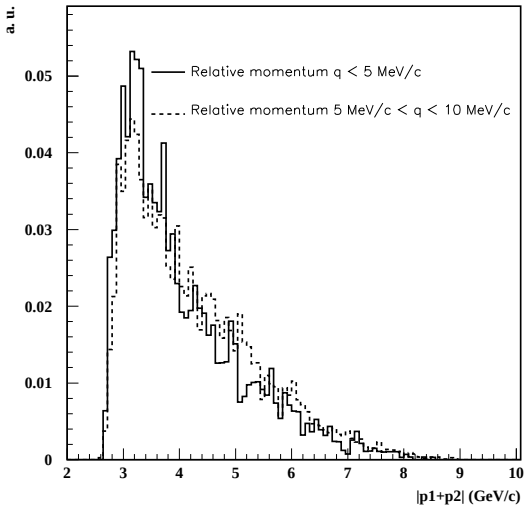

Fig. 2. *Comparison of real pairs momentum distribution weighted with E/PP_t. Two different cases are shown, the solid line refers to low relative momenta and the dashed line to high ones. Data corresponds to the Nickel target.*

interaction. We then calculate the momentum spectrum of these pairs ($|\mathbf{p}_1 + \mathbf{p}_2|$) weighted with the E/PP_t factor[2] for those pairs with relative momentum lower than 5 MeV/c and compared it with the spectrum for those pairs with a relative momentum higher than 5 MeV/c (see Fig. 2). This comparison shows that the pion double inclusive cross-section does not depend strongly on the relative momentum and that an estimate of the spectrum at zero relative momentum can be made with such a cut[3]. In particular, the influence of Coulomb interaction in the $|\mathbf{p}_1 + \mathbf{p}_2|$ spectrum is very small, and can be neglected.

However, since pionium is created only from short-lived sources of $\pi^+\pi^-$ pairs and all sources (short-lived and long-lived) are present in the real data, we need to evaluate the ratio between both sources. As explained in appendix B this ratio was obtained by making use of the FRITIOF hadron Monte Carlo and it can be seen in Fig. 3. The real pionium spectrum is obtained multiplying the solid spectrum of Fig. 2 times the spectrum of Fig. 3. The resulting distribution is shown in Fig. 4.

[2] The resulting distribution would be proportional to:

$$\text{Spectrum from DIRAC data} \propto \int \frac{E}{PP_t} \frac{\mathrm{d}\sigma}{\mathrm{d}P\mathrm{d}\theta\mathrm{d}P\mathrm{d}\theta}\mathrm{d}\theta \qquad (4)$$

[3] This study is only preliminary and a deeper analysis should be made.

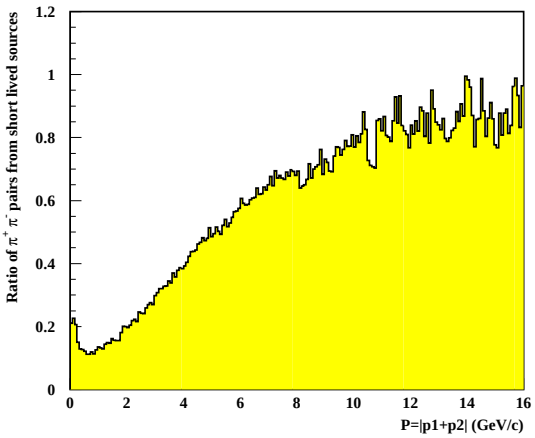

Fig. 3. *Ratio of $\pi^+\pi^-$ pairs from short-lived sources in Nickel.*

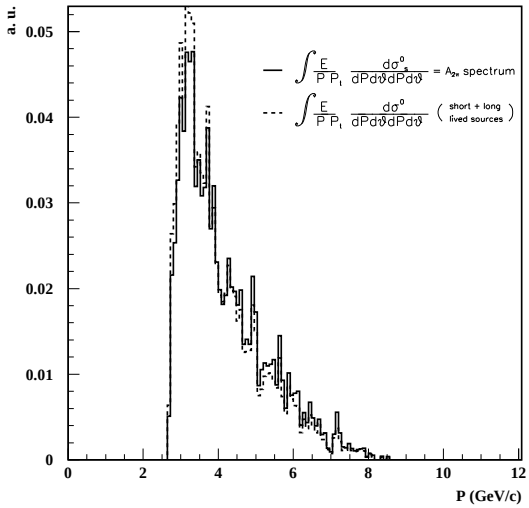

Fig. 4. *Pionium spectrum compared with the weighted double inclusive cross-section. Both spectra from a Nickel target.*

With the initial spectrum of pionium, the relative weight $1/n^3$ for the initial s bound states, and considering that the atoms are randomly created all along the target width [4] we have all the ingredients for the description of the initial parameters of atoms in the creation stage of our Monte Carlo method.

[4] This is because the nuclear interaction length is much larger than the width of the targets of DIRAC experiment.

3 The atom transport through the target

Once the atoms have been created they propagate inside the target material. This propagation is determined by pionium interactions with target nuclei and annihilation probability. Collisions with orbital electrons can be neglected [6].

After a collision with a target nuclei, the atom may excite into a bound state (the corresponding cross-section for these events indicated by the symbol $\sigma_{nlm}^{n'l'm'}$) or ionize into the continuum (for which the cross-section symbol will be σ_{nlm}^{ion}). The total electromagnetic cross-section interaction is related to the discrete-discrete transitions and the ionization cross-section by:

$$\sigma_{nlm}^{total} = \sigma_{nlm}^{ion} + \sum_{n'=0}^{\infty} \sum_{l'=0}^{n'-1} \sum_{m'=-l'}^{l'} \sigma_{nlm}^{n'l'm'}. \tag{5}$$

The electromagnetic collisions will therefore compete with the annihilation process via the $\pi^+ + \pi^- \rightarrow \pi^0 + \pi^0$ channel.

The total probability of pionium-target collisions is well described by the first Born approximation total cross-section [6] [4] given by:

$$\sigma_{nlm}^{\text{total}} = \frac{1}{2\pi\beta^2} \int_0^{\infty} \left|\tilde{U}(\mathbf{q})\right|^2 (1 - F_{nlm}^{nlm}(\mathbf{q}))q\mathrm{d}q, \tag{6}$$

which quantifies the probability for a pionium state nlm to undergo an electromagnetic interaction with a target nuclei.

In particular the probability of discrete-discrete excitation ($nlm \rightarrow n'l'm'$) is given by the cross-section [4]:

$$\sigma_{nlm}^{n'l'm'} = \frac{1 - (-1)^{l-l'}}{\pi\beta^2} \int_0^{\infty} \left|\tilde{U}(\mathbf{q})\right|^2 \left|F_{nlm}^{n'l'm'}\left(\frac{\mathbf{q}}{2}\right)\right|^2 q\mathrm{d}q \tag{7}$$

In equations (6) and (7) $\mathbf{q}$ is the momentum transfer to the scattered atom, β its velocity, and the functions $F_{nlm}^{n'l'm'}(\mathbf{q})$ are called atomic form factors which are defined as:

$$F_{nlm}^{n'l'm'}(\mathbf{q}) = \int \psi_{n'l'm'}^*(\mathbf{r}) e^{i\mathbf{qr}} \psi_{nlm}(\mathbf{r})\mathrm{d}\mathbf{r} \tag{8}$$

where the $\psi_{nlm}(\mathbf{r})$, $\psi_{n'l'm'}(\mathbf{r})$ are the hydrogen-like wave functions of the atom in the initial and final states respectively.

These form factors have been calculated analytically [6] and we have incorporated the corresponding expressions into our Monte Carlo code.

The form factors between discrete states and continuum states have not been calculated in such a useful way[5]. It has been only recently that direct results of ionization cross-sections have been obtained and the analysis of direct calculations for the ionization probabilities will be published shortly [9].

The function $\tilde{U}(\mathbf{q})$ is the Fourier Transform of the Molière parametrization of the Thomas-Fermi potential $U(\mathbf{r})$:

$$\tilde{U}(\mathbf{q}) = 8\pi Z \left(\frac{0.35}{q^2+\beta_1^2} + \frac{0.55}{q^2+\beta_2^2} + \frac{0.10}{q^2+\beta_3^2} \right) \ (E_\pi a_\pi^3) \tag{9}$$

$$U(\mathbf{r}) = \frac{Z}{2r} \left(0.35 e^{-\beta_1 r} + 0.55 e^{-\beta_2 r} + 0.10 e^{-\beta_3 r} \right) \ E_\pi \ ^6 \tag{10}$$

with

$$\beta_1 = \tfrac{0.3 Z^{1/3}}{0.855 a_0} \quad \beta_2 = 4\beta_1 \quad \beta_3 = 5\beta_2, \tag{11}$$

where $a_0 = .52910^{-10}\ m$ is the Bohr radius of Hydrogen atom. Of course this kind of parametrisation allows us to change easily the target material.

Once we have been able to calculate the interaction cross-sections we will try to solve the differential equation system that describes the evolution of the atoms in the target.

$$\frac{\mathrm{d}p_{nlm}(s)}{\mathrm{d}s} = \sum_{n'l'm'} a_{nlm}^{n'l'm'} p_{n'l'm'}(s), \tag{12}$$

where p_{nlm} are the different states population, and s is the distance travelled by the atom in the target. The $a_{nlm}^{n'l'm'}$ are the different transition probabilities per unit of length and are directly related to the transition cross-sections by:

$$a_{nlm}^{n'l'm'} = \frac{\sigma_{nlm}^{n'l'm'} \rho N_0}{A}, \tag{13}$$

[5] Actually there is a complete calculation of hydrogen-like form factors in [10] but they are described in a group theory formalism which makes it unavailable for practical uses.

[6] E_π is the Rydeberg energy for $A_{2\pi}$ atom, which corresponds to 1.86 keV

if $nlm \neq n'l'm'$ and by:

$$a_{nlm}^{nlm} = -\frac{\sigma_{nlm}^{total}\rho N_0}{A} - \begin{cases} 2m_\pi/Pc\tau_{n00} \text{ for nS states,} \\ 0 \qquad\qquad\quad \text{otherwise;} \end{cases} \tag{14}$$

if we talk about a diagonal element of the $a_{nlm}^{n'l'm'}$ matrix. In these equations ρ is the density of the target material, A its atomic weight and N_0 the Avogadro number. In equation (14) P is the atom momentum, τ_n is the lifetime for the corresponding nS state, c is the speed of light and m_π the pion mass.

The lifetime for the different s states of pionium is related by [1]:

$$\tau_{n00} = \tau_{100} n^3 \tag{15}$$

where τ_{100} is the lifetime of $1s$ state. This lifetime is the unknown we shall measure in DIRAC and which we will relate to a direct measurable magnitude, the breakup probability.

As a first corollary of equation (14) we can calculate the mean free path (λ) of pionium in the target:

$$\frac{1}{\lambda} = \frac{1}{\lambda_{anh}} + \frac{1}{\lambda_{int}} = \frac{\sigma_{nlm}^{total}\rho N_0}{A} + \begin{cases} \frac{M}{P\tau_{nlm}} \text{ if } l = 0; \\ 0 \qquad \text{Other case.} \end{cases} \tag{16}$$

So, the probability for an atom to travel a distance x inside the target and then interact in a region of width dx is given by:

$$p(x)\mathrm{d}x = \frac{1}{\lambda} e^{-\frac{x}{\lambda}} \mathrm{d}x, \tag{17}$$

which is the equation in which we will base the transport stage of our Monte Carlo calculation of the breakup probability.

Some calculated values of mean free paths are given in Table 1.

4 The Monte Carlo algorithm.

Once we can simulate the creation and transport of pionium in the target we will be able to solve the equation system (12) by means of the following algorithm:

nlm	λ	nlm	λ	nlm	λ
100	1.06	320	1.50	42±2	0.32
200	2.02	32±2	0.88	43±1	0.59
21±1	2.95	400	0.33	43±3	0.39
300	0.72	41±1	0.30	500	0.18
31±1	0.71	420	0.53	51±1	0.16

Table 1
Mean free path, in μm, for some pionium bound states. Lorentz $\gamma = 2^{1/2}$.

- We take the atom in its initial state specified by the values of $\mathbf{P}_i$ and $\mathbf{R}_i$ [7] as described in Section 2, and generate a free path, x, according to equation (17).
- We displace the atom the length x:

$$\mathbf{R}_{i+1} = x\frac{\mathbf{P}_i}{P_i} + \mathbf{R}_i. \tag{18}$$

- We check that Z_{i+1} is less than the target thickness and, if this is true, we choose between all the possible final states, either annihilation, ionization or discrete-discrete transition between states according to the relative probabilities given by [8]:

$$\frac{\sigma_{nlm}^{n'l'm'}\rho N_{\mathrm{Av}}}{\mathcal{C}A} \tag{19}$$

for discrete-discrete transition,

$$\frac{\sigma_{nlm}^{ion}\rho N_{\mathrm{Av}}}{\mathcal{C}A} \tag{20}$$

for ionization and,

$$\frac{M}{\mathcal{C}P\tau_{nlm}} \tag{21}$$

for annihilation (where P is the atom momentum).
- Annihilation and ionization are final processes, whereas if we have a transition between bound states the atoms continue to travel and we must start again the evolution procedure.

The results of the Monte Carlo program can be obtained in an evident and natural way. From an initial sample of atoms we can calculate how many of

[7] The subscript i refers to the step number in the evolution algorithm.

[8] $\mathcal{C} = \frac{\sigma_{nlm}^{\mathrm{total}}\rho N_{\mathrm{Av}}}{A} + \frac{M}{P\tau_{nlm}}$

them ionize, and hence the breakup probability (P_{br}), how many are annihilated, and hence the annihilation probability (P_{anh}) and how many leave the target in a discrete state, and hence the discrete probability (P_{dsc}). In any of these three cases we can extract relevant information like the atom coordinates, its final state before ionization or annihilation or the state in which it enters in the vacuum after the target.

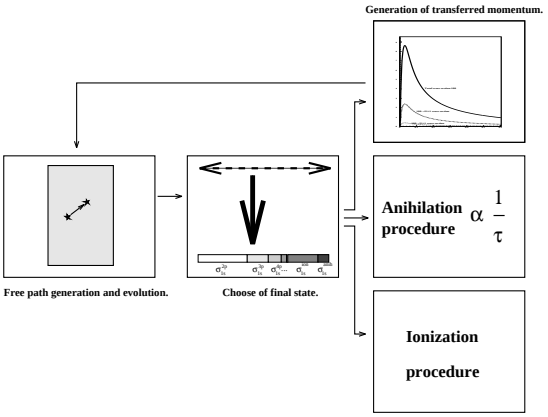

Fig. 5. *Evolution algorithm.*

5 Some comments on the calculation procedure.

Two main difficulties must be avoided in order to make a precise calculation of the breakup probability (P_{br}). The first one refers to the absence of a direct calculation of ionization cross-sections. The second problem is linked with the fact of considering only a finite number of states involved to solve the system of equation (12). In all the results that will be presented throughout this note only those states with principal quantum number $n \leq n_{max}$ have been considered. The value of n_{max} can be obviously increased but, of course, some cut must be finally applied. Therefore the result on P_{br} must be obtained in some indirect way which will be described below.

As a first consequence of these problems we will not be able to make a direct calculation of the amount of ionized atoms. Since the best approach for us to ionization cross-sections is:

$$\sigma_{nlm}^{ion} = \sigma_{nlm}^{total} - \sum_{n'=0}^{n'=\infty} \sum_{l'=0}^{l'=n'-1} \sum_{m'=-l'}^{m'=l'} \sigma_{nlm}^{n'l'm'}, \tag{22}$$

and as we can only perform finite sums we are forced to split this equation as:

$$\sigma_{nlm}^{ion} + \sum_{n'=n_{max}}^{n'=\infty} \sum_{l'=0}^{l'=n'-1} \sum_{m'=-l'}^{m'=l'} \sigma_{nlm}^{n'l'm'} = \sigma_{nlm}^{total} - \sum_{n'=0}^{n'=n_{max}} \sum_{l'=0}^{l'=n'-1} \sum_{m'=-l'}^{m'=l'} \sigma_{nlm}^{n'l'm'}. \tag{23}$$

	Tail or Ionized atoms				Annihilated atoms				Surviving atoms			
n_{max}	7	8	9	10	7	8	9	10	7	8	9	10
$n = 1$	97147	96736	95890	95244	488592	488109	488002	488086	100172	99444	98535	98015
$n = 2$	51180	49711	48578	47757	4972	4925	4938	4851	19610	19492	19549	19148
$n = 3$	34542	32234	30976	30128	254	238	225	258	6841	6966	6804	6710
$n = 4$	30767	27479	25318	24081	25	27	33	32	3244	3199	3212	3217
$n = 5$	33750	27077	23897	21667	9	11	8	4	1824	1846	1813	1838
$n = 6$	43580	30177	24371	20996	3	2	1	1	1209	1115	1168	1121
$n = 7$	81261	39784	27829	22496	1	1	2	1	1080	759	732	714
$n = 8$	-	69962	35914	25670	-	-	1	-	-	709	566	518
$n = 9$	-	-	61134	32990	-	-	-	-	-	-	504	400
$n = 10$	-	-	-	53483	-	-	-	-	-	-	-	304
Total	372227	373160	373907	374512	493856	493313	493210	493232	133980	133530	132883	131985

Table 2
Results for an initial sample of 10^6 *atoms. The principal quantum number n, before the atom becomes into the indicated final situation, is indicated. A Nickel target of 95 μm and non-monochromatic pionic atoms were considered.*

This relation means that we will not be able to distinguish between those atoms which are ionized and those that suffer a transition between a discrete state involved in the calculation (hence with $n < n_{max}$) and a discrete state with $n > n_{max}$. So one additional hypothesis on the calculation of P_{tail}, the probability for the atom to remain in a discrete state with $n > n_{max}$ after the target, will be needed to perform the P_{br} calculation. This will be discussed in the next section.

Considering that the evolution of any atom is finished if the atom is ionized, annihilated, if it is excited into a state with $n > n_{max}$ or if it leaves the target in a discrete state with $n < n_{max}$. Hence the probabilities for any of these final events are related by:

$$1 = P_{br} + P_{anh} + P_{dsc} + P_{tail}, \tag{24}$$

therefore the limitation on the direct calculation of P_{br} can be avoided if we transform this equation into:

$$P_{br} = 1 - (P_{anh} + P_{dsc} + P_{tail}), \tag{25}$$

but the reliability on P_{anh} and on P_{dsc} must be proved.

To test the stability of the obtained results on P_{dsc} and P_{anh} we have filled Table 2 for several calculations in which n_{max} was scanned from 7 to 10.

From Table 2 we can conclude that P_{anh} is almost unchanged with n_{max}. Furthermore the number of annihilated atoms from states with $n > 6$ is completely negligible. The same conclusion can be made on discrete state atoms. The result becomes stable for those states with $n < (n_{max} - 2)$.

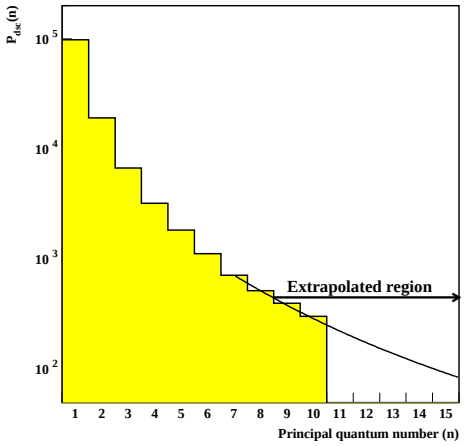

Fig. 6. *Example of a tail fit result. A Nickel 95. μm width target and a lifetime of 3. fs for pionium were considered.*

Therefor the calculation of P_{tail} is the remaining problem to be solved and to this task we dedicate the next section.

6 Tail analysis.

As explained above the amount of atoms excited to discrete states with $n > n_{max}$, the so called *discrete atoms tail*, are involved [9] in the calculation of P_{br}.

In order to calculate the total amount of atoms in this tail and, as suggested in [1], we have fitted the results for $P_{dsc}(n)$ for $n = (n_{max} - 3)$ and $n = (n_{max} - 2)$ to an expression of the type:

$$P_{dsc}(n) = \frac{a}{n^3} + \frac{b}{n^5}. \tag{26}$$

Hence, we have estimated the value of P_{tail} making the summation of (26) from $n = (n_{max} - 1)$ to ∞. Fig. 6 shows the fit for the results of Table 2.

[9] Meanwhile the tail for annihilated atoms is negligible as can be seen in Table 2

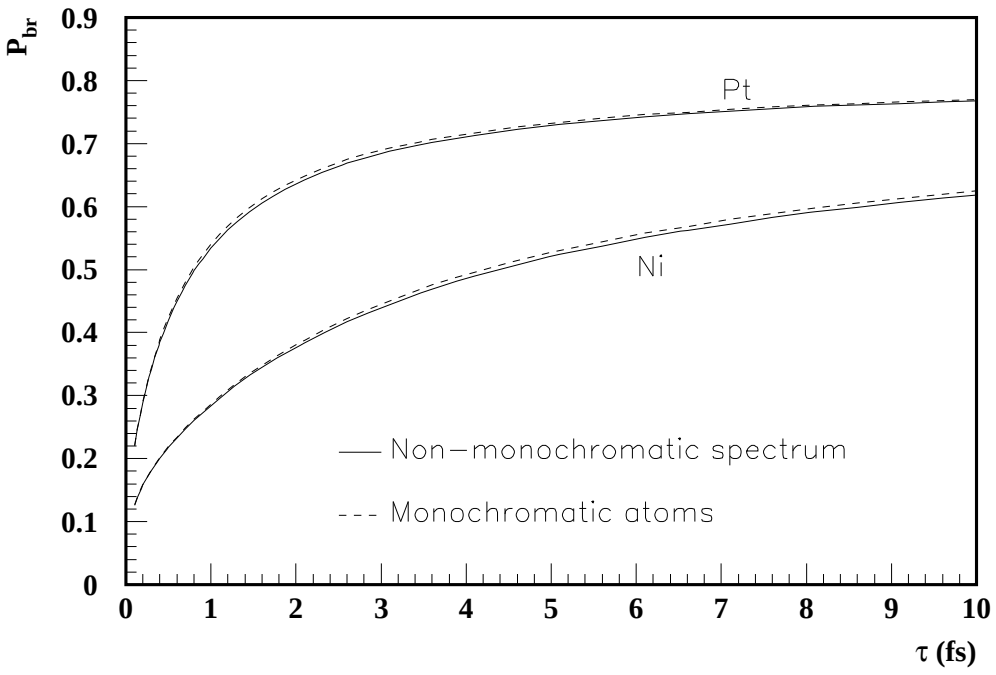

Fig. 7. *Comparison of P_{br} as a function of lifetime for monochromatic and non-monochromatic atoms. The upper curves correspond to a 22.3 μm Pt target and the lower to a 95. μm Ni target. the monochromatic samples were produced with 4.160 GeV/c in the case of the Nickel target and 4.233 for the Platinum target.*

7 Results on breakup probability.

7.1 Results on $P_{br}(\tau)$.

The initial spectrum of Fig. 4 was considered to obtain the $P_{br}(\tau)$ curve of Fig. 7 for a Nickel target of 95 μm width. The resulting curve is compared with the result for monochromatic atoms at the average momentum of the same spectrum (4.233 GeV/c). The observed differences are very small (within 1%) and become slightly larger as τ increases.

The same procedure was applied for a Platinum target of 22.3 μm width. In this case the mean momentum of pionic atoms was found to be 4.160 GeV/c.

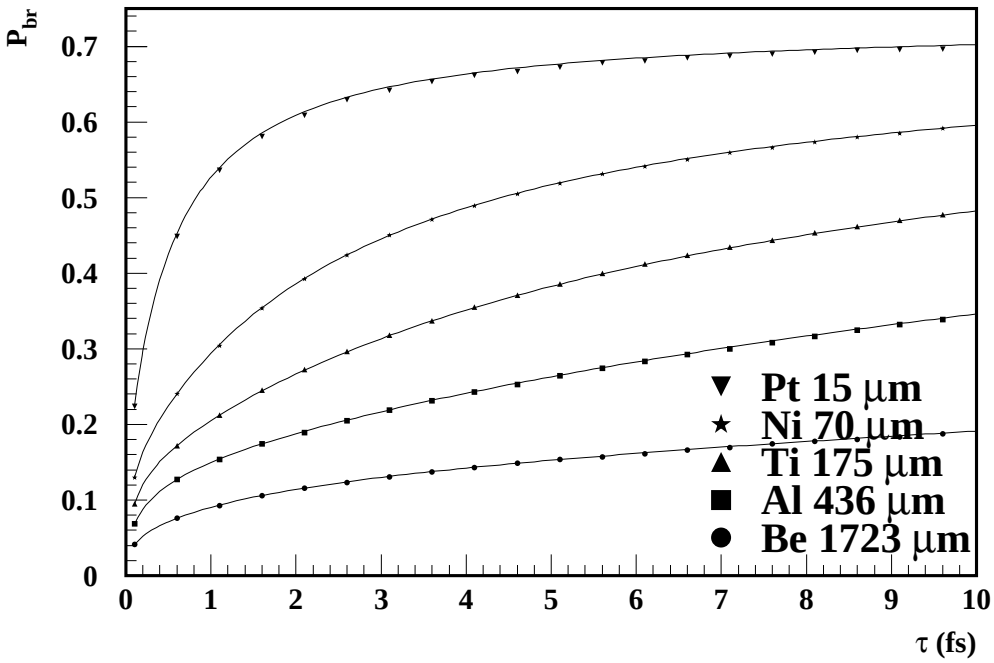

Fig. 8. *Comparison of results. The solid lines are those of Ref.* [7] *and the points are those calculated with the Monte Carlo method. Monochromatic atoms of 4.7 GeV/c momentum were considered.*

7.2 Some comparisons.

In Fig. 8 the obtained results on P_{br} are presented for several targets. The comparison with the calculations of [7] which are displayed as solid lines show an excellent agreement within 1%. In Table 3, P_{br}, the breakup probability and

$$\delta P_{br} = \frac{1}{P_{br}} \frac{\mathrm{d}P_{br}}{\mathrm{d}\tau} \tag{27}$$

are compared between this work and Ref. [7]. This magnitude (δP_{br}) has a large relevance because it is the maximum allowed uncertainty for a P_{br} measurement to reach a 10% precision in the measurement of pionium lifetime. Also ΔP_{br}, the difference between the results on P_{br} for [7] and this work is shown in Table 3.

	Z	S μm	P_{br}	P_{br} Ref. [7]	δP_{br}	δP_{br} Ref. [7]	ΔP_{br}
Be	04	2585.	0.132	0.133	$3.2\ 10^{-2}$	$3.2\ 10^{-2}$	$1.\ 10^{-3}$
Al	13	654.2	0.222	0.222	$3.6\ 10^{-2}$	$3.7\ 10^{-2}$	$< 1.\ 10^{-3}$
Ti	22	263.1	0.326	0.325	$4.0\ 10^{-2}$	$4.1\ 10^{-2}$	$-1.\ 10^{-3}$
Fe	26	129.9	0.432	0.435	$3.5\ 10^{-2}$	$3.8\ 10^{-2}$	$3.\ 10^{-3}$
Ni	28	104.3	0.470	0.471	$3.3\ 10^{-2}$	$3.5\ 10^{-2}$	$1.\ 10^{-3}$
Cu	29	105.2	0.465	0.470	$3.4\ 10^{-2}$	$3.5\ 10^{-2}$	$5.\ 10^{-3}$
Mo	42	70.2	0.537	0.541	$2.8\ 10^{-2}$	$3.0\ 10^{-2}$	$4.\ 10^{-3}$
Ta	73	30.0	0.666	0.672	$1.4\ 10^{-2}$	$1.7\ 10^{-2}$	$6.\ 10^{-3}$
Re	75	23.3	0.694	0.699	$1.2\ 10^{-2}$	$1.4\ 10^{-2}$	$5.\ 10^{-3}$
Pt	78	22.3	0.699	0.704	$1.1\ 10^{-2}$	$1.3\ 10^{-2}$	$5.\ 10^{-3}$

Table 3
Comparison of results. S means target thickness.

8 Conclusions.

A prediction for the $P_{br}(\tau)$ function for DIRAC experimental conditions has been made. The stability of this result is better than 2% for the different variations discussed throughout the note.

Acknowledgements.

I am indebt with professors B. Adeva and M. Plo for their stimulating suggestions and discussions. Special thanks are due to L.G. Afanasyev and to J.J. Saborido for their help.

A Calculation of pionium production cross-section.

In this appendix we are going to describe how to obtain equation (3) starting from equation (1).

Let us take the result:

$$\frac{\mathrm{d}\sigma^A(n,l,m)}{\mathrm{d}\mathbf{P}} = (2\pi)^3 \frac{E}{M_A} |\psi_{nlm}(\mathbf{0})|^2 \frac{\mathrm{d}\sigma_s^0}{\mathrm{d}\mathbf{p}_{\pi^+}\mathrm{d}\mathbf{p}_{\pi^-}} \qquad \text{(A.1)}$$

if we now consider spherical coordinates this equation is transformed into:

$$\frac{1}{P^2\sin(\theta)}\frac{\mathrm{d}\sigma^A(n,l,m)}{\mathrm{d}P\mathrm{d}\theta\mathrm{d}\phi} = \tag{A.2}$$
$$(2\pi)^3\frac{E}{M_A}|\psi_{nlm}(\mathbf{0})|^2\frac{1}{p_{\pi^+}^2\sin(\theta_{\pi^+})}\frac{1}{p_{\pi^-}^2\sin(\theta_{\pi^-})}\frac{\mathrm{d}\sigma_s^0}{\mathrm{d}p_{\pi^+}\mathrm{d}\theta_{\pi^+}\mathrm{d}\phi_{\pi^-}\mathrm{d}p_{\pi^-}\mathrm{d}\theta_{\pi^-}\mathrm{d}\phi_{\pi^-}}$$

but as $\mathbf{P} = 2\mathbf{p}_{\pi^+} = 2\mathbf{p}_{\pi^-}$ we have that $P = 2p_{\pi^+} = 2p_{\pi^-}$, $\theta = \theta_{\pi^+} = \theta_{\pi^-}$ and $\phi = \phi_{\pi^+} = \phi_{\pi^-}$ we can make the corresponding substitutions and obtain:

$$\frac{\mathrm{d}\sigma^A(n,l,m)}{\mathrm{d}P\mathrm{d}\theta\mathrm{d}\phi} = 2^6(2\pi)^3\frac{E}{M_A}|\psi_{nlm}(\mathbf{0})|^2\frac{1}{P^2\sin(\theta)}\frac{\mathrm{d}\sigma_s^0}{\mathrm{d}P\mathrm{d}\theta\mathrm{d}\phi\mathrm{d}P\mathrm{d}\theta\mathrm{d}\phi} \tag{A.3}$$

As we have axial symmetry around the ϕ angle we can eliminate the dependence on it and as $P\sin(\theta) = P_t$ we can write the desired final expression as:

$$\frac{\mathrm{d}\sigma^A(n,l,m)}{\mathrm{d}P\mathrm{d}\theta} = |\psi_{nlm}(\mathbf{0})|^2\frac{2^6(2\pi)^3}{M_A}\frac{E}{PP_t}\frac{\mathrm{d}\sigma_s^0}{\mathrm{d}P\mathrm{d}\theta\mathrm{d}P\mathrm{d}\theta}. \tag{A.4}$$

The relevance on this expression is given by the fact that it gives us the weight E/PP_t with which we can link an estimation of the double inclusive cross-section and the pionium production.

B How to obtain the spectrum only from short-lived sources.

As shown in [1], pionic atoms are bound states of $\pi^+\pi^-$ pairs from short-lived sources. These sources are characterized by a range of pion formation of $r_{form} \sim 1fm$, much less than the Bohr radius of pionium ($a_\pi = 387fm$). Hence, as direct data shown in Fig. 2 does not distinguish between those pairs from short or long lived sources, we need to extract, as a function of the center of mass momentum, which is the rate of these type of sources from the complete sample.

Therefore we can define $f(P,\theta)$ as:

$$\frac{\mathrm{d}\sigma_s^0}{\mathrm{d}\mathbf{p}_{\pi^+}\mathrm{d}\mathbf{p}_{\pi^-}} = f(P,\theta)\frac{\mathrm{d}\sigma^0}{\mathrm{d}\mathbf{p}_{\pi^+}\mathrm{d}\mathbf{p}_{\pi^-}} \tag{B.1}$$

In order to calculate $f(P,\theta)$ we have considered the relation between semi-inclusive and inclusive cross-sections given by:

$$\frac{\mathrm{d}\sigma_s^0}{\mathrm{d}\mathbf{p}_{\pi^+}\mathrm{d}\mathbf{p}_{\pi^-}} = \frac{F_s(\mathbf{p}_{\pi^+},\mathbf{p}_{\pi^-})}{\sigma_{\mathrm{inelastic}}}\frac{\mathrm{d}\sigma_s^+}{\mathrm{d}\mathbf{p}_{\pi^+}}\frac{\mathrm{d}\sigma_s^-}{\mathrm{d}\mathbf{p}_{\pi^-}} \tag{B.2}$$

$$\frac{\mathrm{d}\sigma^0}{\mathrm{d}\mathbf{p}_{\pi^+}\mathrm{d}\mathbf{p}_{\pi^-}} = \frac{F(\mathbf{p}_{\pi^+},\mathbf{p}_{\pi^-})}{\sigma_{\mathrm{inelastic}}}\frac{\mathrm{d}\sigma^+}{\mathrm{d}\mathbf{p}_{\pi^+}}\frac{\mathrm{d}\sigma^-}{\mathrm{d}\mathbf{p}_{\pi^-}} \tag{B.3}$$

where $F_s(\mathbf{p}_{\pi^+},\mathbf{p}_{\pi^-})$ and $F(\mathbf{p}_{\pi^+},\mathbf{p}_{\pi^-})$ are the correlation functions *due only to strong interaction*, for the case of only short-lived sources and for the complete double inclusive cross-section. The value $\sigma_{inelastic}$ corresponds to the inelastic cross-section of hadron production in $proton - target$ collisions.

Hence if we define $f^+(P,\theta)$ and $f^-(P,\theta)$ as:

$$\frac{\mathrm{d}\sigma_s^+}{\mathrm{d}\mathbf{p}_{\pi^+}} = f^+(P,\theta)\frac{\mathrm{d}\sigma^+}{\mathrm{d}\mathbf{p}_{\pi^+}} \tag{B.4}$$

$$\frac{\mathrm{d}\sigma_s^-}{\mathrm{d}\mathbf{p}_{\pi^-}} = f^-(P,\theta)\frac{\mathrm{d}\sigma^-}{\mathrm{d}\mathbf{p}_{\pi^-}} \tag{B.5}$$

we can see that:

$$f(P,\theta) = \frac{F_s(\mathbf{p}_{\pi^+},\mathbf{p}_{\pi^-})}{F(\mathbf{p}_{\pi^+},\mathbf{p}_{\pi^-})}f^+(P,\theta)f^-(P,\theta). \tag{B.6}$$

As explained in [1] the correlation functions depend only on the relative momentum of the pair. Therefore, as $\mathbf{p}_{\pi^+} = \mathbf{p}_{\pi^-}$ they remain constant and only produce an scaling factor between f and f^+f^-.

Furthermore, as the angular aperture in DIRAC spectrometer is small (about 5 mrad.), we can forget about the angular dependence on θ in expression (B.4) to conclude that:

$$f(P) \propto f^+(P)f^-(P). \tag{B.7}$$

We have calculated f^+ and f^- from the momentum spectra of Fig. B.1 from the FRITIOF hadronic Monte Carlo. And from this calculation we have obtained the result on $f(P)$ shown in Fig. 3.

C Tabulated results with the comparison results.

In Table C.1 this work results are compared with those of Ref. [1]. These comparison was also shown in Fig. 8.

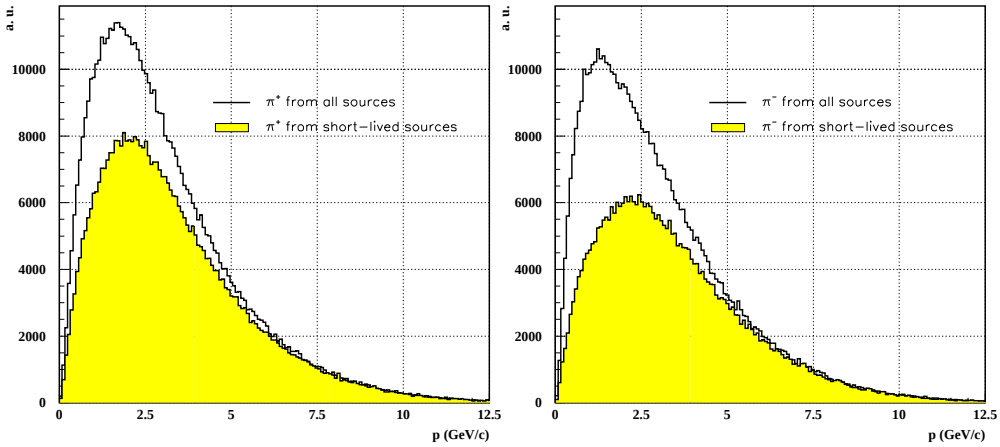

Fig. B.1. *Spectra for π^+ and π^- for the total yield of these particles and for short-lived sources only. The spectra refers to a Nickel target and considers* DIRAC *geometrical acceptance.*

References

[1] B. Adeva et al., *Proposal to the SPSLC: Lifetime measurement of $\pi^+\pi^-$ atoms to test low energy QCD predictions*, CERN/SPSLC/P 284 (1994).

[2] C. Santamarina, *A física dos átomos piónicos*, Diploma thesis, Universidade de Santiago de Compostela.

[3] L.L. Nemenov, *Elementary Relativistic Atoms*, Yad. Fiz., **41** (1985) 980.

[4] S. Mrówczyński, *Interaction of Elementary Atoms with Matter*, Phys. Rev., **A33** (1986) 1549.

[5] H.A. Bethe and E.E. Salpeter, *Quantum Mechanics of One- and Two-Electron Atoms*, Plenum Publishing Corporation, (1977).

[6] L.G. Afanasyev and A.V. Tarasov, *Breakup of Relativistic $\pi^+\pi^-$ Atoms in Matter*, Yad. Fiz., **59** (1996) 2212; Phys. At. Nuc., **59** (1996) 2130.

[7] L.G. Afanasyev, *Comments on a choice of the target material*, Results presented to DIRAC in the February 1998 collaboration meeting.

[8] Particle Data Group, *Review of Particle Physics*, Eur. Phys. Jour., **C3** (1998) 1.

[9] L.G. Afanasyev and C. Santamarina, *More on Breakup probability.* To be published as a DIRAC internal note.

[10] A.O. Barut and R. Wilson, *Analytic Group-theoretical Form Factors of Hydrogenlike Atoms for Discrete and Continuum Transitions*, Phys. Rev., **A40** (1978) 1967.

Table C.1

Comparison of results on P_{br} for several material and lifetime values

Z	04 Be		13 Al		22 Ti		28 Ni		78 Pt	
thick μm	1723.359		436.229		175.401		69.536		14.895	
τ (fs)	This work	Ref. [1]	This work	Ref. [1]	This work	Ref. [1]	This work	Ref. [1]	This work	Ref. [1]
0.5	7.091E-02	7.130E-02	1.192E-01	1.196E-01	1.622E-01	1.622E-01	2.234E-01	2.244E-01	4.202E-01	4.253E-01
1.0	8.958E-02	9.039E-02	1.488E-01	1.496E-01	2.058E-01	2.052E-01	2.929E-01	2.941E-01	5.217E-01	5.269E-01
1.5	1.024E-01	1.037E-01	1.696E-01	1.706E-01	2.391E-01	2.384E-01	3.437E-01	3.457E-01	5.724E-01	5.781E-01
2.0	1.134E-01	1.140E-01	1.862E-01	1.878E-01	2.664E-01	2.666E-01	3.843E-01	3.861E-01	6.036E-01	6.089E-01
2.5	1.217E-01	1.226E-01	2.019E-01	2.029E-01	2.916E-01	2.914E-01	4.169E-01	4.186E-01	6.238E-01	6.294E-01
3.0	1.287E-01	1.299E-01	2.155E-01	2.166E-01	3.130E-01	3.134E-01	4.440E-01	4.453E-01	6.373E-01	6.440E-01
3.5	1.353E-01	1.364E-01	2.282E-01	2.293E-01	3.338E-01	3.333E-01	4.664E-01	4.676E-01	6.488E-01	6.549E-01
4.0	1.412E-01	1.423E-01	2.391E-01	2.412E-01	3.513E-01	3.512E-01	4.854E-01	4.866E-01	6.582E-01	6.635E-01
4.5	1.466E-01	1.476E-01	2.497E-01	2.524E-01	3.679E-01	3.676E-01	5.010E-01	5.028E-01	6.645E-01	6.703E-01
5.0	1.511E-01	1.526E-01	2.609E-01	2.629E-01	3.824E-01	3.825E-01	5.151E-01	5.169E-01	6.704E-01	6.758E-01
5.5	1.565E-01	1.572E-01	2.704E-01	2.730E-01	3.966E-01	3.962E-01	5.283E-01	5.292E-01	6.753E-01	6.804E-01
6.0	1.599E-01	1.616E-01	2.801E-01	2.826E-01	4.094E-01	4.089E-01	5.382E-01	5.400E-01	6.775E-01	6.844E-01
6.5	1.646E-01	1.658E-01	2.898E-01	2.917E-01	4.207E-01	4.205E-01	5.482E-01	5.497E-01	6.825E-01	6.877E-01
7.0	1.689E-01	1.698E-01	2.973E-01	3.004E-01	4.326E-01	4.313E-01	5.565E-01	5.583E-01	6.853E-01	6.906E-01
7.5	1.727E-01	1.736E-01	3.064E-01	3.088E-01	4.416E-01	4.414E-01	5.638E-01	5.661E-01	6.863E-01	6.932E-01
8.0	1.764E-01	1.773E-01	3.149E-01	3.168E-01	4.515E-01	4.508E-01	5.717E-01	5.731E-01	6.896E-01	6.954E-01
8.5	1.798E-01	1.809E-01	3.218E-01	3.245E-01	4.600E-01	4.595E-01	5.783E-01	5.795E-01	6.917E-01	6.974E-01
9.0	1.827E-01	1.844E-01	3.292E-01	3.319E-01	4.673E-01	4.677E-01	5.833E-01	5.853E-01	6.934E-01	6.992E-01
9.5	1.863E-01	1.877E-01	3.368E-01	3.390E-01	4.760E-01	4.753E-01	5.895E-01	5.906E-01	6.949E-01	7.008E-01
10.0	1.890E-01	1.910E-01	3.423E-01	3.459E-01	4.840E-01	4.825E-01	5.945E-01	5.955E-01	6.960E-01	7.022E-01